Journal of Cardiovascular Computed Tomography 13 (2019) 219–225

Contents lists available at ScienceDirect

Journal of Cardiovascular Computed Tomography

journal homepage: www.elsevier.com/locate/jcct

Research paper

Effect of tube potential and luminal contrast attenuation on atherosclerotic plaque attenuation by coronary CT angiography: In vivo comparison with intravascular ultrasound

Hidenari Matsumoto[a,*], Satoshi Watanabe[b], Eisho Kyo[b], Takafumi Tsuji[b], Yosuke Ando[b], Yuka Otaki[a], Sebastien Cadet[a], Piotr J. Slomka[a], Daniel S. Berman[a,c], Damini Dey[d], Balaji K. Tamarappoo[a,c]

[a] Department of Imaging, Cedars-Sinai Medical Center, Los Angeles, CA, USA
[b] Department of Cardiology, Kusatsu Heart Center, Kusatsu, Shiga, Japan
[c] The Heart Institute, Cedars-Sinai Medical Center, Los Angeles, CA, USA
[d] Biomedical Imaging Research Institute, Cedars-Sinai Medical Center, Los Angeles, CA, USA

ARTICLE INFO

Keywords:
Coronary computed tomography angiography
Plaque characterization
Tube potential
Intravascular ultrasound

ABSTRACT

Background: It has been shown that CT attenuation of noncalcified plaques depends on luminal contrast attenuation (LCA). Although tube potential (kilovolt [kV]) has been shown to exert influence on plaque attenuation through LCA as well as its direct effects, in-vivo studies have not investigated plaque attenuation at lower tube potentials less than 120 kV. We sought to evaluate the effect of kV and LCA on thresholds for lipid-rich and fibrous plaques as defined by intravascular ultrasound (IVUS).

Methods: CT attenuation of IVUS-defined plaque components (lipid-rich, fibrous, and calcified plaques) were quantified in 52 consecutive patients with unstable angina, who had coronary CT angiography performed at 100 kV (n = 25) or 120 kV (n = 27) using kV-adjusted contrast protocol prior to IVUS. CT attenuation of plaque components was compared between the two groups.

Results: LCA was similar in the 100-kV and 120-kV groups (417.6 ± 83.7 Hounsfield Units [HU] vs 421.3 ± 54.9 HU, p = 0.77). LCA correlated with CT attenuation of lipid-rich (r = 0.49, p = 0.001) and fibrous plaques (r = 0.32, p < 0.05), but not with that of calcified plaques (r = 0.04, p = 0.81). When plaque attenuation was normalized to LCA, lipid-rich (0.087 ± 0.036, range −0.012–0.147) and fibrous plaque attenuation (0.234 ± 0.056, range 0.153–0.394) were distinct (p < 0.001) with no overlap for both kV groups. CT attenuation was not significantly different between 100-kV and 120-kV groups for lipid-rich (34.0 ± 21.5 vs 39.3 ± 12.9, p = 0.33) or fibrous plaques (95.4 ± 19.1 vs 97.6 ± 22.0, p = 0.75).

Conclusion: Plaque attenuation thresholds for non-calcified plaque components should be adjusted based on LCA. Further adjustment may not be required for different tube potentials.

1. Introduction

Plaque rupture is a key event leading to acute coronary syndromes.[1–3] Autopsy studies and intravascular ultrasound (IVUS) have shown that plaque rupture occurs most often in plaque containing lipid-rich necrotic core.[2,4–7] Coronary computed tomography (CT) angiography (CTA) can differentiate among lipid-rich, noncalcified, and calcified plaque components and can be used to identify high-risk plaque features.[4,8–11]

On CTA, a high-risk plaque with a lipid-rich necrotic core is identified by its low attenuation.[4,8–11] The generally accepted threshold of < 30 Hounsfield Units (HU) for low attenuation plaque (LAP) was derived from CTA performed at a peak tube potential of 135 kV (kV).[10,12] Subsequent CTA studies of high-risk plaque have used this threshold for defining LAP regardless of the tube potential used during image acquisition. The burden of noncalcified plaque (NCP) on CTA, including the fibrous plaque defined by IVUS, has been associated with increased cardiac events.[13] Plaque attenuation thresholds of 30–150 HU have been used to define NCP,[12,14] and these have been correlated with IVUS.[10]

* Corresponding author. 8700 Beverly Boulevard, Los Angeles, CA, 90048, USA.
E-mail address: Hidenari.Matsumoto@cshs.org (H. Matsumoto).

https://doi.org/10.1016/j.jcct.2019.02.004
Received 18 September 2018; Received in revised form 8 November 2018
Available online 12 February 2019

Abbreviations

CTA	coronary computed tomography angiography
CT	computed tomography
HU	Hounsfield Units
IVUS	intravascular ultrasound
kV	kilovolt
LAP	low attenuation plaque
LCA	luminal contrast attenuation
NCP	noncalcified plaque

Lowering tube potential is a potent strategy to reduce radiation dose.[15] Since the degree of contrast enhancement is increased by lower tube potentials,[16] lower kV settings are also employed as an approach to reduce the amount of contrast media.[17] Several studies reported that plaque attenuation from CTA depends on luminal contrast opacification.[18–20] Therefore, lower kV settings can affect plaque attenuation through luminal contrast opacification.

Thus far, to our knowledge, in-vivo studies have not investigated plaque attenuation for LAP and NCP at lower tube potentials less than 120 kV. We sought to evaluate the effect of different tube potentials (100 and 120 kV) and luminal contrast attenuation on CT attenuation of plaque components (lipid-rich, fibrous, and calcified plaques) as defined by IVUS as the reference standard.

2. Methods

2.1. Patients

This retrospective study included consecutive patients with unstable angina who underwent a clinically indicated CTA followed by IVUS within a period of 1 week at Kusatsu Heart Center (Kusatsu, Shiga, Japan) from November 2009 to December 2012. The study protocol was approved by the local ethics committee, and written informed consent was obtained from all patients for the use of their data for research. Patients underwent CTA for anginal symptoms without elevation of troponin. Unstable angina was defined as one of the following: 1) prolonged (> 20 min) symptom at rest; 2) new onset angina with Canadian Cardiovascular Society class ≥ 2; 3) recent destabilization of previously stable angina with Canadian Cardiovascular Society Class ≥ 3.[21,22] Patients with coronary artery bypass surgery, poor image quality on CTA or IVUS, stented lesions or predilatation before IVUS examination were excluded.

2.2. Image acquisition

2.2.1. IVUS

All IVUS examinations were performed prior to percutaneous coronary intervention in a standard fashion with commercially available 40-MHz imaging catheters (Boston Scientific Corporation, Minneapolis, MN, USA or Terumo Co., Tokyo, Japan) as described previously.[23] The imaging catheter was advanced beyond the distal portion of the target lesion for percutaneous coronary intervention, and automated pullback was performed at a rate of 0.5 mm/s.

2.2.2. CTA

CTA images were acquired with a 64-detector scanner (Lightspeed VCT, GE Healthcare, Milwaukee, Wisconsin, USA). All patients received nitroglycerin for coronary vasodilation, and those with a heart rate over 60 beats per minute were given beta-blockers unless a contraindication was present. An intravenous bolus of iopamidol (Iopamiron 370, Schering) was continuously injected at the same rate for 10–12 s, depending on the scan length, followed by a 20:80 admixture of contrast agent (25 ml). The injection rate of contrast agent was adjusted according to body weight and tube potential (Table 1).[17,24–26]

Table 1
Contrast injection protocols.

Body weight (kg)	Injection rate (ml/sec)	
	100 kV	120 kV
< 40	2.3	2.7
40–45	2.5	3.0
45–50	2.7	3.3
50–55	3.0	3.6
55–60	3.3	3.9
60–65	3.6	4.2
65–70	N/A	4.5
70–75	N/A	4.8
75–80	N/A	5.0
80–85	N/A	5.3
≥85	N/A	5.6

kV = kilovolt; N/A = not applicable.

Retrospectively ECG-gated helical scan was performed with ECG-based tube current modulation. Patients with body mass index ≤25 kg/m^2 and body weight ≤65 kg were scanned with the 100 kV protocol (100-kV group, n = 25), and the others were scanned with the 120 kV protocol (120-kV group, n = 27). The scan parameters were collimation of 64 × 0.625-mm, rotation time of 350 msec, and tube current of 500–780 mAs. Transaxial images were reconstructed with a half-scan and filtered backprojection reconstruction algorithm at the cardiac phase exhibiting minimal cardiac motion. Image reconstruction parameters comprised the individually adapted field of view, matrix size of 512 × 512 pixels, section thickness of 0.625 mm, and a medium-soft tissue convolution kernel.

2.3. Data analysis

2.3.1. IVUS analysis

IVUS images were analyzed using dedicated software (echoPlaque, INDEC Medical Systems, Santa Clara, California, USA) by consensus between two experienced observers, who were blinded to the result of CTA. Lipid-rich, fibrous, and calcified plaques were identified using the following criteria as reported previously.[6,23] Lipid-rich plaques included hypoechoic plaques with ultrasonic attenuation and absence of bright calcium. Fibrous plaques were defined as atheroma with echogenicity similar to the adventitia without attenuation, echolucency, or acoustic shadowing. Calcified plaques were defined as hyperechoic plaques with acoustic shadowing. The arcs of attenuation and acoustic shadowing were measured in degrees with a protractor centered on the lumen.

2.3.2. Quantitative CTA analysis

CTA images were analyzed by experienced observers using dedicated software (AutoPlaque 2.0, Cedars-Sinai Medical Center, Los Angeles, California, USA).[27] Curved multiplanar reconstruction and cross-sectional images were used to compare IVUS images. We selected representative cross-sectional IVUS images where each plaque component (lipid-rich, fibrous, or calcified plaque) was most significant and homogeneous. For lipid-rich and fibrous plaques, cross-sectional slices with calcification were excluded from the analysis. CT images were matched to IVUS by anatomical landmarks, including the distance from the aorto-coronary ostium, side branches, or calcifications. Multiple regions of interest (3–5 depending on the size of plaque) were placed within the corresponding plaque component to quantify HU. The size of region-of-interest was 0.2 × 0.2 mm. Luminal contrast attenuation for each plaque was defined as the mean HU of proximal and distal luminal reference points.[9] In 10 lipid-rich, fibrous, and calcified plaques, the mean HU values were measured in two cross-sectional images ≤1 mm apart from each other in the same lesion.

2.4. Statistical analysis

Statistical analysis was performed with SPSS Statistics 24 (IBM Corporation, Armonk, New York, USA). Data were expressed as means ± standard deviations for quantitative variables and as frequencies with percentages for categorical variables. Between-group comparisons were made with the unpaired-samples *t*-test or Mann-Whitney *U* test for quantitative variables and with the χ^2 test or Fisher's exact test for categorical variables, where appropriate. The receiver-operating characteristic analysis was used to determine the optimal cutoff HU values for discriminating between lipid-rich and fibrous plaques. Correlations between HU values of each plaque component and luminal contrast attenuation were assessed with Pearson's correlation coefficient. Intraobserver and interobserver variability for the HU values of plaques were examined in randomly selected 20 patients using Bland-Altman analysis and intraclass correlation coefficient. A p-value < 0.05 was considered a statistically significant difference.

3. Results

3.1. Clinical characteristics and image quality

Clinical characteristics and image quality are listed in Tables 2 and 3, respectively. Intra-arterial contrast opacification was not significantly different between the two kV groups. Sufficient intra-arterial opacification (> 250 HU in the proximal coronary artery)[15] was achieved in all the patients (mean: 431.2 ± 67.0; range: 255.7–613.0).

3.2. IVUS findings

A total of 124 cross-sections consisting of 41 lipid-rich plaques (18 and 23 in the 100-kV and the 120-kV groups, respectively), 39 fibrous plaques (18 and 21 in the 100-kV and the 120-kV groups, respectively), and 44 calcified plaques (20 and 24 in the 100-kV and the 120-kV groups, respectively) were analyzed. There were no significant differences in arcs of ultrasonic attenuation and calcification on the corresponding IVUS images between the 100-kV and 120-kV groups (arc of attenuation: 119.6 ± 32.3° and 115.3 ± 43.5°, p = 0.55; arc of calcification; 113.3 ± 41.7° and 105.8 ± 42.3°, p = 0.56). Fig. 1 shows representative images of each plaque component.

3.3. Influence of luminal contrast enhancement on plaque attenuation

Fig. 2 displays scatter plots of plaque HU and luminal contrast attenuation. Luminal contrast attenuation correlated with HU of lipid-rich (r = 0.49, p = 0.001) and fibrous plaques (r = 0.32, p < 0.05), but not with that of calcified plaques (r = 0.04, p = 0.81). Although the mean HU was significantly lower in lipid-rich plaques than in fibrous plaques in both kV groups (p < 0.001), there was an overlap in the distribution of HU values between lipid-rich (mean 37.0 ± 17.2, 95% confidence interval [CI] 31.6–42.4, range −4.5–74.6) and fibrous plaques (mean 96.6 ± 20.5, 95% CI 89.9–103.2, range 61.9–149.7) (Figs. 3A and 4A). On the receiver-operating characteristic curve analysis, the optimal cutoff value for discriminating between lipid-rich and fibrous plaques was 58 HU. When plaque attenuation was normalized to luminal contrast attenuation (plaque/lumen HU ratio), lipid-rich and fibrous plaque attenuation were distinct (p < 0.001) with no overlap (lipid-rich: mean 0.087 ± 0.036, 95% CI 0.075–0.098, range −0.012–0.147; fibrous: mean 0.234 ± 0.056, 95% CI 0.216–0.252, range 0.153–0.394) (Fig. 3B).

3.4. HU at different kV settings

The mean HU values of IVUS-defined plaque components at the two different kV settings are summarized in Fig. 4. The mean HU values in the 100-kV vs 120-kV groups were similar for lipid-rich (34.0 ± 21.5 vs 39.3 ± 12.9, p = 0.33) and fibrous plaques (95.4 ± 19.1 vs 97.6 ± 22.0, p = 0.75). The mean HU of calcified plaque was increased at 100 kV vs 120 kV (1006.7 ± 217.2 vs 791.4 ± 213.7, p < 0.01).

3.5. Reproducibility

The intraclass correlation coefficients for intraobserver and interobserver variability of mean HU value were: lipid-rich, 0.963 and 0.912; fibrous, 0.870 and 0.863; calcified, 0.981 and 0.990, respectively (p < 0.001 for all). By Bland-Altman analysis, the average differences in HU value (with the limits of agreement) for intraobserver and interobserver measurements were: lipid-rich, 0.6 (± 9.2) and 1.6 (± 14.4); fibrous, 3.4 (± 18.1) and −3.3 (± 23.7); calcified, −18.0 (± 93.4) and 13.3 (± 70.1), respectively.

3.6. Mean HU of plaque components in adjacent cross-sections

Between adjacent cross-sections, there were no significant differences in HU value of IVUS-defined lipid-rich (32.4 ± 14.3 vs 31.5 ± 11.5, p = 0.80), fibrous (94.2 ± 18.2 vs 97.0 ± 27.5, p = 0.68), and calcified plaques (1090.6 ± 152.8 vs 1116.0 ± 165.0, p = 0.56). By Bland-Altman analysis, the mean differences in HU value were 1.0, −2.8, and −25.4, and the limits of agreement were ± 22.4, ± 41.3, and ± 262.5 for lipid-rich, fibrous, and calcified plaques, respectively.

4. Discussion

In this study, evaluating HU of lipid-rich, fibrous and calcified plaques at two different tube potentials, we have demonstrated the following findings: 1) Attenuation of noncalcified plaques is significantly related to that for luminal contrast attenuation; 2) There are overlaps in the raw distribution of lipid-rich and fibrous plaque attenuation; however, when plaque attenuation is normalized to that of lumen, such overlaps do not persist, allowing identification of these NCP components; 3) No significant differences in HU values for lipid-rich and fibrous plaques are observed between 100 kV and 120 kV under the condition of similar luminal contrast attenuation.

Plaque features observed on CTA have been associated with increased risk of cardiac events, including the presence and volume of LAP and NCP.[12–14,28] IVUS, which can differentiate high-risk plaque components, has been used as the gold standard in studies that have examined the effect of lipid-lowering treatment on plaque composition and plaque burden.[29] Previous studies have demonstrated a strong correlation between these high-risk plaque features characterized by IVUS and CTA.[4,8–11]

Table 2
Clinical characteristics and scan conditions.

	100 kV	120 kV	p value
	(n = 25)	(n = 27)	
Clinical characteristics			
Age, yrs	69 ± 11	63 ± 11	0.11
Male, n (%)	17 (68)	25 (93)	< **0.05**
Weight, kg	52.9 ± 10.0	66.8 ± 8.0	< **0.001**
Body mass index, kg/m^2	20.9 ± 2.5	25.0 ± 1.7	< **0.001**
Mean heart rate, beats/min	56 ± 6	55 ± 4	0.33
Hypertension, n (%)	16 (64)	21 (78)	0.27
Diabetes mellitus, n (%)	7 (28)	10 (37)	0.49
Dyslipidemia, n (%)	13 (52)	13 (48)	0.78
Current smoking, n (%)	5 (20)	5 (19)	0.89
Target vessel (LAD/LCX/RCA), n	14/2/9	17/4/6	0.48

LAD: left anterior descending coronary artery; LCX = left circumflex coronary artery; LM = left main; RCA, right coronary artery.

Table 3
Quantitative parameters from coronary CT angiography.

	100 kV	120 kV	p value
Intra-arterial opacification			
Aorta, HU	454.5 ± 76.6	431.8 ± 52.6	0.22
Proximal coronary artery, HU	433.3 ± 76.0	429.3 ± 58.9	0.83
Lumen across plaque			
Lipid-rich plaque, HU	413.7 ± 72.0	427.5 ± 58.4	0.54
Fibrous plaque, HU	413.5 ± 85.5	426.3 ± 56.4	0.58
Calcified plaque, HU	424.6 ± 94.9	411.0 ± 50.9	0.57
All, HU	417.6 ± 83.7	421.3 ± 54.9	0.77

HU = Hounsfield unit; kV = kilovolt.

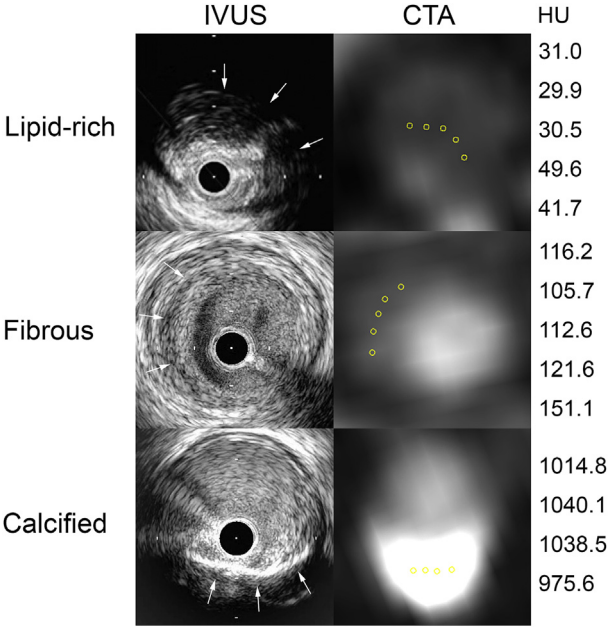

Fig. 1. Examples of IVUS-defined plaque components with corresponding cross-sectional CTA images.
CTA = coronary computed tomography angiography; HU = Hounsfield unit; IVUS = intravascular ultrasound.

NCP characterization based on absolute HU values is widely accepted in clinical practice as well as research studies.[4,8,12–14,28] A potential limitation of NCP characterization based on absolute HU values is that HU of NCP is dependent on luminal contrast opacification.[18–20] Our results are consistent with previous reports, which show that luminal contrast attenuation strongly influences the measured attenuation of LAP and NCP.[18–20] In the present study, HU values of lipid-rich and fibrous plaques were correlated with luminal contrast attenuation. In vulnerable plaques, the lipid core which has the lowest HU value among plaque components and is often separated from the lumen by a thin fibrous cap.[2,4] Due to partial volume effect, attenuation of LAP may be strongly affected by luminal contrast attenuation. It, therefore, becomes important to take luminal contrast attenuation into account when evaluating plaque composition based on plaque attenuation. We also argue that fixed HU threshold values for lipid-rich and fibrous plaques cannot be applied when comparing plaque composition between different CTA studies unless luminal contrast attenuation is similar between images. In fact, the mean attenuation of lipid-rich plaque in the present study (mean 37.0 ± 17.2; range −4.5–74.6) was higher than what has been reported (mean 10.6 ± 11.6; range -15–33) in landmark studies using 135 kV.[10,12] This discrepancy could be attributed to the difference in luminal contrast attenuation between the previous study (mean 258; range 174–384)[10] and ours (mean 420; range 245–640). A higher threshold for LAP has also been proposed by other investigators. In a study comparing ex-vivo CTA performed at 120 kV with histologic plaque characterization, Han et al. found 75 HU to be the reliable cut-off for LAP with high diagnostic accuracy and agreement with lipid-rich plaque area on histology. It is important to note that the attenuation of luminal contrast attenuation in their study (mean 444; range 201–725) was similar to that for our data.

Given the importance of luminal contrast attenuation on HU of NCP and LAP, we sought to achieve a similar luminal contrast attenuation in our CTA at both 100 kV and 120 kV using the combined body weight and kV-adjusted iodine injection protocol in a manner similar to Kok et al.[25] In a comparative study between 100-kV and 120-kV tube potentials using the same contrast injection protocol, the HU of coronary artery was 16% higher in the 100-kV setting despite a comparable body size.[30] Kok et al. validated in a phantom study that similar luminal contrast attenuation can be achieved at both 100 kV and 120 kV using a 12% lower iodine load and iodine delivery rate for 100 kV imaging compared to image acquisition at 120 kV.[17] Using the individually tailored contrast protocol, similar luminal contrast attenuation was achieved at the different kV settings in the present study.

Since there are a number of patient-related and CT scanning-related factors affecting contrast enhancement,[16] variations in luminal contrast attenuation cannot be fully controlled even with the use of body weight and kV-adjusted contrast protocol. In line with prior reports, the distribution of mean HU value partially overlapped between lipid-rich and fibrous plaques in the current study.[9,31] Interestingly, when plaque HU normalized to luminal contrast attenuation was applied, lipid-rich and fibrous plaque components were discriminated clearly with no overlap. The finding also supports the effect of luminal contrast attenuation on

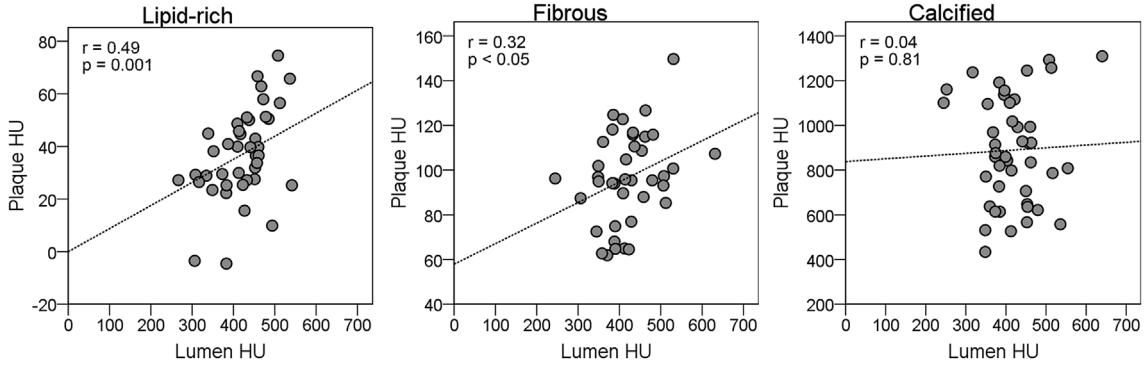

Fig. 2. Correlation between attenuation values of plaque components and lumen.
Scatter plots demonstrate correlations between luminal contrast attenuation and plaque HU for each component defined by IVUS on CTA scanned with either 100 kV or 120 kV protocol. Luminal contrast attenuation correlated with HU of non-calcified plaques, but not with that of calcified plaques.
Abbreviations as in Fig. 1.

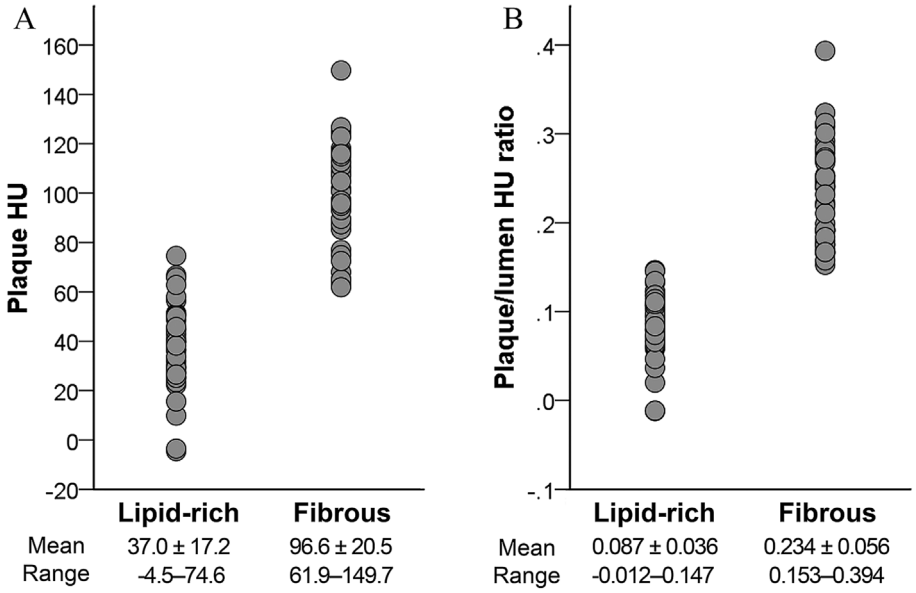

Fig. 3. Distribution of absolute HU and plaque/lumen HU ratio for lipid-rich and fibrous plaques
(A) Absolute HU value
(B) Plaque/lumen HU ratio
The overlap between lipid-rich and fibrous plaques is not seen when absolute HU of plaque components is indexed for luminal contrast attenuation.
An abbreviation as in Fig. 1.

plaque attenuation of LAP and NCP. Plaque characterization based on luminal contrast attenuation-adjusted plaque HU may, therefore, be a plausible option to facilitate comparison in longitudinal studies or to minimize discrepancies between studies due to different methodologies.

The Society of Cardiovascular Computed Tomography guideline recommends low kV acquisitions to reduce radiation dose,[15] and choice of 100-kV over 120-kV tube potential is most commonly used for CTA.[32,33] However, the thresholds for LAP and NCP have not been assessed with different tube potentials and have been adopted in studies irrespective of tube potential used during CTA. In the present in-vivo study with contrast, we did not find significant differences in HU of IVUS-defined lipid-rich and fibrous plaques between patients who underwent CTA at 100 kV and patients who underwent CTA at 120 kV, with similar luminal contrast enhancement to each other. The highest changes between low and high energies are in more dense tissues such as iodinated contrast and calcium, due to a higher likelihood of photoelectric interaction in dense tissue at lower x-ray energies; signals from less dense tissues such as non-calcified plaque and adipose tissue show less change.[34] An ex-vivo study using human cadaver heart specimens at different tube potentials without contrast has also demonstrated that lower tube potentials increased HU of calcified plaques, whereas the differences in HU of histology-verified lipid-rich and fibrous plaques were minimal.[35] Therefore, tube potential may have little direct impact on plaque attenuation of NCP and LAP as long as luminal contrast attenuation is similar.

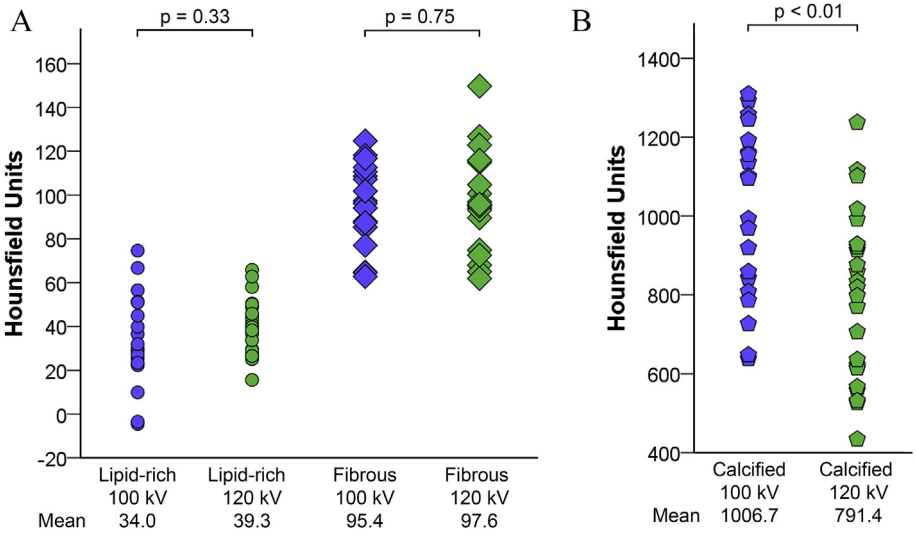

Fig. 4. Comparison of HU values for IVUS-defined plaque components between the 100-kV and 120-kV settings.
(A) Noncalcified plaque
(B) Calcified plaque
kV = kilovolt; other abbreviation as in Fig. 1.

4.1. Clinical implications

Measurement of the burden of LAP and NCP with sequential CTA is increasingly being utilized for noninvasive assessment of the effects of medical therapy. Since lower tube potentials in CTA are associated with lower effective radiation dose, the 100-kV protocol is now being widely adopted for clinical practice.[32] Our results emphasize the need for an individually tailored contrast protocol at different kV settings in order to reduce the variability of luminal contrast attenuation. Our study is also the first to show that there is no overlap between lipid-rich and fibrous plaque attenuation when plaque attenuation is systematically normalized to luminal contrast attenuation.

4.2. Study limitations

We acknowledge several limitations. First, this is a single center retrospective study with a small number of patients who underwent CTA at either 100 kV or 120 kV with an older but 64-slice CT scanner. With newer scanners, images are reconstructed with varying types and levels of iterative reconstruction, which affects plaque attenuation. Therefore, in this study, we used CTA data reconstructed with filtered back projection reconstruction for consistency. Further investigation on differences in thresholds for plaque type is necessary with a larger cohort using the latest scanners and techniques, including different levels of iterative reconstruction. Current CTA software enables volumetric plaque volume measurement and plaque characterization. However, due to the nature of gray-scale IVUS used as the reference standard in this study, we were not able to quantify plaque composition on IVUS. Importantly, most of the patients in our study have extensive echo attenuation on IVUS due to their plaque composition. Extensive echo attenuation precludes accurate plaque volume measurement by IVUS. Therefore, this study focused on plaque HU, which is still widely accepted in clinical practice and research studies; plaque HU could be measured in adjacent cross-sections in CTA in direct concordance with IVUS. The same patients did not undergo CTA at different tube potentials for ethical considerations of added radiation exposure. Lastly, we did not use tube potentials lower than 100 kV due to technical limitations of the scanner.

4.3. Conclusions

Plaque attenuation thresholds for non-calcified plaque components should be adjusted based on luminal contrast attenuation. Further adjustment may not be required for different tube potentials.

Disclosures

Piotr J Slomka, Daniel S Berman, Sebastien Cadet, and Damini Dey received software royalties from Cedars-Sinai Medical Center; Piotr J Slomka, Daniel S Berman, and Damini Dey have a patent.

References

1. Burke AP, Farb A, Malcom GT, Liang YH, Smialek J, Virmani R. Coronary risk factors and plaque morphology in men with coronary disease who died suddenly. *N Engl J Med.* 1997;336(18):1276–1282.
2. Falk E, Nakano M, Bentzon JF, Finn AV, Virmani R. Update on acute coronary syndromes: the pathologists' view. *Eur Heart J.* 2013;34(10):719–728.
3. Virmani R, Kolodgie FD, Burke AP, Farb A, Schwartz SM. Lessons from sudden coronary death: a comprehensive morphological classification scheme for atherosclerotic lesions. *Arterioscler Thromb Vasc Biol.* 2000;20(5):1262–1275.
4. Maurovich-Horvat P, Ferencik M, Voros S, Merkely B, Hoffmann U. Comprehensive plaque assessment by coronary CT angiography. *Nat Rev Cardiol.* 2014;11(7):390–402.
5. Stone GW, Maehara A, Lansky AJ, et al. A prospective natural-history study of coronary atherosclerosis. *N Engl J Med.* 2011;364(3):226–235.
6. Pu J, Mintz GS, Biro S, et al. Insights into echo-attenuated plaques, echolucent plaques, and plaques with spotty calcification: novel findings from comparisons among intravascular ultrasound, near-infrared spectroscopy, and pathological histology in 2,294 human coronary artery segments. *J Am Coll Cardiol.* 2014;63(21):2220–2233.
7. Narula J, Nakano M, Virmani R, et al. Histopathologic characteristics of atherosclerotic coronary disease and implications of the findings for the invasive and noninvasive detection of vulnerable plaques. *J Am Coll Cardiol.* 2013;61(10):1041–1051.
8. Voros S, Rinehart S, Qian Z, et al. Coronary atherosclerosis imaging by coronary CT angiography: current status, correlation with intravascular interrogation and meta-analysis. *JACC Cardiovasc Imaging.* 2011;4(5):537–548.
9. Obaid DR, Calvert PA, Gopalan D, et al. Atherosclerotic plaque composition and classification identified by coronary computed tomography: assessment of computed tomography-generated plaque maps compared with virtual histology intravascular ultrasound and histology. *Circ Cardiovasc Imaging.* 2013;6(5):655–664.
10. Motoyama S, Kondo T, Anno H, et al. Atherosclerotic plaque characterization by 0.5-mm-slice multislice computed tomographic imaging. *Circ J.* 2007;71(3):363–366.
11. Han D, Torii S, Yahagi K, et al. Quantitative measurement of lipid rich plaque by coronary computed tomography angiography: A correlation of histology in sudden cardiac death. *Atherosclerosis.* 2018;275:426–433.
12. Motoyama S, Kondo T, Sarai M, et al. Multislice computed tomographic characteristics of coronary lesions in acute coronary syndromes. *J Am Coll Cardiol.* 2007;50(4):319–326.
13. Hell MM, Motwani M, Otaki Y, et al. Quantitative global plaque characteristics from coronary computed tomography angiography for the prediction of future cardiac mortality during long-term follow-up. *Eur Heart J Cardiovasc Imaging.* 2017;18(12):1331–1339.
14. Motoyama S, Sarai M, Harigaya H, et al. Computed tomographic angiography characteristics of atherosclerotic plaques subsequently resulting in acute coronary syndrome. *J Am Coll Cardiol.* 2009;54(1):49–57.
15. Abbara S, Blanke P, Maroules CD, et al. SCCT guidelines for the performance and acquisition of coronary computed tomographic angiography: a report of the society of cardiovascular computed tomography guidelines committee: endorsed by the North American Society for Cardiovascular imaging (NASCI). *J Cardiovasc Comput Tomogr.* 2016;10(6):435–449.
16. Bae KT. Intravenous contrast medium administration and scan timing at CT: considerations and approaches. *Radiology.* 2010;256(1):32–61.
17. Kok M, Mihl C, Hendriks BM, et al. Optimizing contrast media application in coronary CT angiography at lower tube voltage: evaluation in a circulation phantom and sixty patients. *Eur J Radiol.* 2016;85(6):1068–1074.
18. Cademartiri F, Mollet NR, Runza G, et al. Influence of intracoronary attenuation on coronary plaque measurements using multislice computed tomography: observations in an ex vivo model of coronary computed tomography angiography. *Eur Radiol.* 2005;15(7):1426–1431.
19. Horiguchi J, Fujioka C, Kiguchi M, et al. Soft and intermediate plaques in coronary arteries: how accurately can we measure CT attenuation using 64-MDCT? *AJR Am J Roentgenol.* 2007;189(4):981–988.
20. Dalager MG, Bottcher M, Andersen G, et al. Impact of luminal density on plaque classification by CT coronary angiography. *Int J Cardiovasc Imaging.* 2011;27(4):593–600.
21. Thygesen K, Alpert JS, Jaffe AS, et al. Third universal definition of myocardial infarction. *J Am Coll Cardiol.* 2012;60(16):1581–1598.
22. Roffi M, Patrono C, Collet JP, et al. ESC guidelines for the management of acute coronary syndromes in patients presenting without persistent ST-segment elevation: task force for the management of acute coronary syndromes in patients presenting without persistent ST-segment elevation of the European society of Cardiology (ESC). *Eur Heart J.* 2015;37(3):267–315 2016.
23. Mintz GS, Nissen SE, Anderson WD, et al. American college of cardiology clinical expert consensus document on standards for acquisition, measurement and reporting of intravascular ultrasound studies (IVUS). A report of the American college of cardiology task force on clinical expert consensus documents. *J Am Coll Cardiol.* 2001;37(5):1478–1492.
24. Nakaura T, Awai K, Yauaga Y, et al. Contrast injection protocols for coronary computed tomography angiography using a 64-detector scanner: comparison between patient weight-adjusted- and fixed iodine-dose protocols. *Invest Radiol.* 2008;43(7):512–519.
25. Tatsugami F, Matsuki M, Inada Y, et al. Feasibility of low-volume injections of contrast material with a body weight-adapted iodine-dose protocol in 320-detector row coronary CT angiography. *Acad Radiol.* 2010;17(2):207–211.
26. Mihl C, Kok M, Altintas S, et al. Evaluation of individually body weight adapted contrast media injection in coronary CT-angiography. *Eur J Radiol.* 2016;85(4):830–836.
27. Dey D, Cheng VY, Slomka PJ, et al. Automated 3-dimensional quantification of noncalcified and calcified coronary plaque from coronary CT angiography. *J Cardiovasc Comput Tomogr.* 2009;3(6):372–382.
28. Motoyama S, Ito H, Sarai M, et al. Plaque characterization by coronary computed tomography angiography and the likelihood of acute coronary events in mid-term follow-up. *J Am Coll Cardiol.* 2015;66(4):337–346.
29. Nicholls SJ, Ballantyne CM, Barter PJ, et al. Effect of two intensive statin regimens on progression of coronary disease. *N Engl J Med.* 2011;365(22):2078–2087.
30. Zhang C, Zhang Z, Yan Z, Xu L, Yu W, Wang R. 320-row CT coronary angiography: effect of 100-kV tube voltages on image quality, contrast volume, and radiation dose. *Int J Cardiovasc Imaging.* 2011;27(7):1059–1068.
31. Marwan M, Taher MA, El Meniawy K, et al. In vivo CT detection of lipid-rich coronary artery atherosclerotic plaques using quantitative histogram analysis: a head to head comparison with IVUS. *Atherosclerosis.* 2011;215(1):110–115.
32. Min JK, Dunning A, Lin FY, et al. Age- and sex-related differences in all-cause mortality risk based on coronary computed tomography angiography findings results from the International Multicenter CONFIRM (Coronary CT Angiography Evaluation

for Clinical Outcomes: an International Multicenter Registry) of 23,854 patients without known coronary artery disease. *J Am Coll Cardiol.* 2011;58(8):849–860.
33. Chang HJ, Lin FY, Lee SE, et al. Coronary atherosclerotic precursors of acute coronary syndromes. *J Am Coll Cardiol.* 2018;71(22):2511–2522.
34. McCollough CH, Leng S, Yu L, Fletcher JG. Dual- and multi-energy CT: principles, technical approaches, and clinical applications. *Radiology.* 2015;276(3):637–653.
35. Tanami Y, Ikeda E, Jinzaki M, et al. Computed tomographic attenuation value of coronary atherosclerotic plaques with different tube voltage: an ex vivo study. *J Comput Assist Tomogr.* 2010;34(1):58–63.